Structure of the Bovine Antimicrobial Peptide Indolicidin Bound to Dodecylphosphocholine and Sodium Dodecyl Sulfate Micelles[†,‡]

Annett Rozek, Carol L. Friedrich, and Robert E. W. Hancock*

Department of Microbiology and Immunology, University of British Columbia, #300-6174 University Boulevard, Vancouver, British Columbia V6T 1Z3, Canada

Received March 29, 2000; Revised Manuscript Received September 28, 2000

ABSTRACT: Indolicidin is a cationic, 13-residue antimicrobial peptide (ILPWKWPWWPWRR-NH_2) which is unusually rich in tryptophan and proline. Its antimicrobial action involves the bacterial cytoplasmic membrane. Fluorescence and circular dichroism spectra demonstrated the structural similarity of indolicidin in complexes with large unilamellar phospolipid vesicles and with detergent micelles. The structure of indolicidin bound to zwitterionic dodecylphosphocholine (DPC) and anionic sodium dodecyl sulfate (SDS) micelles was determined using NMR methods and shown to represent a unique membrane-associated peptide structure. The backbone structure in DPC, well defined between residues 3 and 11, was extended, with two half-turns at residues Lys-5 and Trp-8. The backbone structure in SDS, well defined between residues 5 and 11, was also extended, but lacked the bend in the C-terminal half. Indolicidin in complexes with DPC had a central hydrophobic core composed of proline and tryptophan, which was bracketed by positively charged regions near the peptide termini. The tryptophan side chains, with one exception, folded flat against the peptide backbone, thus giving the molecule a wedge shape. Indolicidin in complexes with SDS had an arrangement of hydrophobic and cationic regions similar to that found in the presence of DPC. The tryptophan side chains were less well defined than for indolicidin in DPC and extended away from the peptide backbone. The preferred location of indolicidin in DPC micelles and lipid bilayers, analyzed using spin-label probes, was at the membrane interface.

Cationic antimicrobial peptides play a key role in the host defense system of many higher organisms such as plants, insects, amphibians, and mammals (*1*). On the basis of their rapid killing action, often within minutes of contact with microbes, cationic peptides have been suggested to constitute the first line of defense against invading bacteria, viruses, and fungi (*2*). With the alarming emergence of pathogens, which are resistant against conventional antibiotics, cationic peptides are under intense research aimed at developing a novel class of antimicrobial drugs. Most structures determined to date have included β-sheet peptides and amphipathic α-helical peptides (*3*). However, few structures have been determined for other classes of cationic peptides, such as extended peptides that are rich in proline, arginine, or aromatic amino acids. A recent example is tritrpticin, although this peptide has a relatively weak antimicrobial activity (*4*).

Indolicidin is a linear antimicrobial peptide isolated from the cytoplasmic granules of bovine neutrophils (*5*). The 13-amino acid sequence (ILPWKWPWWPWRR-NH_2) contains the highest fraction of tryptophan (39%) ever observed for a protein sequence. Indolicidin has a broad spectrum of antimicrobial activity against Gram-positive and Gram-negative bacteria (*5*), protozoa (*6*), fungi (*7*), and the enveloped virus HIV-1 (*8*). The antibacterial action of indolicidin is thought to involve interaction with the cytoplasmic membrane. The peptide readily partitions into phospholipid bilayers with a fraction of >95% bound to lipid and compromises membrane integrity (*9*−*11*). Indolicidin is able to form small, transient conductance increases in planar lipid bilayers and partially depolarize the cytoplasmic membrane potential gradient of bacteria (*11*). However, exactly how such a short peptide does this is as yet unknown, and we initiated the current study in the hope of providing some insight into this process.

The previous structural analysis of indolicidin, based on CD spectroscopic data, has been somewhat controversial. While an unordered structure was detected in aqueous solution (*10*), either a poly-L-proline type II helix (*10*) or a β-turn conformation was proposed for the lipid-bound molecule (*9, 12*). We have determined the structure of indolicidin by nuclear magnetic resonance (NMR)[1] spectroscopy using detergent micelles, a widely used lipid model system for the structural study of membrane binding peptides or proteins by solution NMR methods (*13*). Detergent micelles tumble faster in solution than the large phospholipid vesicles, resulting in narrower NMR signals and, consequently, higher spectral resolution, which enables the determination of detailed three-dimensional peptide structures. Our CD and fluorescence data suggested that the conformation

[†] This work was supported by grants from the Canadian Bacterial Diseases Network and the Canadian Cystic Fibrosis Foundation. A.R. and R.E.W.H. hold a fellowship and Distinguished Scientist Award, respectively, from the Medical Research Council of Canada.

[‡] The coordinates and NMR restraints of indolicidin in DPC and SDS micelles have been deposited at the RCSB Protein Databank, entries 1G89 and 1G8C, respectively.

* To whom correspondence should be addressed. Phone: (604) 822-2682. Fax: (604) 822-6041. E-mail: bob@cmdr.ubc.ca.

10.1021/bi000714m CCC: $19.00
Published on Web 12/19/2000

of indolicidin is similar when bound to phospholipid vesicles or detergent micelles. The structure of indolicidin was determined in two different micelle systems, zwitterionic dodecylphosphocholine (DPC) and anionic sodium dodecyl sulfate (SDS), to examine the effect of headgroup charge on the peptide structure. While both structures share similarities, they each represent a distinct membrane-associated peptide fold, containing elements of both poly-L-proline II helix and β-turn.

MATERIALS AND METHODS

Indolicidin (ILPWKWPWWPWRR-NH_2) was synthesized by the Nucleic Acid/Peptide Synthesis (NAPS) facility at the University of British Columbia. The peptide was pure as confirmed by HPLC and mass spectroscopy. SDS was obtained from Fischer Scientific (Fair Lawn, NJ). DPC-d_{38}, SDS-d_{25}, and D_2O were purchased from Cambridge Isotope Laboratories (Andover, MA). POPC and POPG were purchased from Northern Lipids Inc. (Vancouver, BC). Headgroup-labeled tempo-PC, 5-doxyl-PC, and 12-doxyl-PC were obtained from Avanti Polar Lipids Inc. (Alabaster, AL), while 5-doxylstearic acid, 16-doxylstearic acid, and methanol-d_4 were obtained from Aldrich (Milwaukee, WI).

Preparation of Unilamellar Liposomes. A chloroform solution of lipid was dried under a stream of N_2, followed by desiccation under vacuum, to remove the solvent. The resulting lipid film was rehydrated in 10 mM sodium phosphate buffer (pH 7.0). The suspension was put through five cycles of freezing and thawing, followed by 10-fold extrusion through 0.1 μm double-stacked Poretics filters (AMD Manufacturing Inc., Mississauga, ON) using an extruder device (Lipex Biomembranes, Vancouver, BC).

Fluorescence Spectroscopy. Fluorescence emission spectra were recorded on an LS 50B spectrofluorimeter [Perkin-Elmer (Canada) Ltd., Markham, ON]. Measurements were performed between 300 and 450 nm at 1 nm increments using a 5 mm quartz cell at room temperature. The excitation wavelength was set to 280 nm with both the excitation and emission slit widths set to 4 nm. Spectra were baseline corrected by subtracting blank spectra of the corresponding lipid or detergent solutions without peptide. The samples contained 2 μM peptide and 0.5 mM lipid or 10 mM detergent in 10 mM HEPES buffer (pH 7.2).

Circular Dichroism Measurements. Circular dichroism (CD) spectra were obtained using a J-720 spectropolarimeter (Japan Spectroscopic Co., Tokyo, Japan). Each spectrum (190−250 nm) was the average of four scans using a quartz cell with a 1 mm path length at room temperature. The scanning speed was 50 nm/min at a step size of 0.1 nm, a 2 s response time, and a 1.0 nm bandwidth. All samples were 50 μM in peptide and 10 mM in sodium phosphate buffer (pH 7.0). The concentration of lipid or detergent was 2 or 10 mM, respectively. Spectra were baseline corrected by subtracting a blank spectrum of a sample containing all components except the peptide. After noise correction, ellipticities were converted to mean residue molar ellipticities [θ] in units of deg cm^2 $dmol^{-1}$.

NMR Spectroscopy. The NMR samples were prepared by adding solutions of perdeuterated SDS or DPC in 10 mM sodium phosphate buffer (pH 5), containing 10% D_2O, to lyophilized indolicidin. The final samples were 2 mM in indolicidin, and 400 and 240 mM in DPC-d_{38} and SDS-d_{25}, respectively.

NMR spectra were recorded on a Bruker AMX600 or Varian Unity500 spectrometer, operating at 600.13 or 499.95 MHz, respectively. One-dimensional spectra were acquired between 25 and 50 °C and between pH 4.0 and 9.4. For two-dimensional spectra, the sample temperature and pH were maintained at 37 °C and 4.7, respectively. Homonuclear TOCSY (*14*), NOESY (*15*), and DQF-COSY (*16*) spectra were acquired. Water suppression was achieved using the WATERGATE technique (*17*, *18*) or by presaturation during the recycling delay (2−2.5 s). Spectra were collected with 512−800 data points in F_1, 2K data points in F_2, and 32−64 transients. TOCSY spectra were acquired using the MLEV-17 pulse sequence (*19*) at spin-lock times of 60 and 75 ms. NOESY spectra were recorded at mixing times between 50 and 150 ms. An additional NOESY spectrum (τ_m = 100 ms) of indolicidin in DPC was obtained at 32 °C to reveal peptide resonances which were overlapped with the water resonance at 37 °C.

To establish the amount of detergent necessary for maximal binding of the peptide, indolicidin was titrated with either DPC-d_{38} or SDS-d_{25} and the chemical shifts at 37 °C were monitored by one-dimensional NMR spectra. Small aliquots of a detergent stock solution were added to indolicidin dissolved in 10 mM phosphate buffer (pH 5) up to a maximal molar peptide:detergent ratio of 1:200. The pH was adjusted to 4.7 after each addition of detergent.

Qualitative exchange rates of labile hydrogen atoms of indolicidin in DPC micelles at 37 °C were determined by dissolving lyophilized indolicidin in D_2O, containing DPC-d_{38} at a molar peptide:detergent ratio of 1:100. The pH* was determined to be 3.7 (uncorrected for the isotope effect). Several one-dimensional NMR spectra were acquired during the first hour after dissolution in D_2O. Then a TOCSY spectrum with a total acquisition time of ~6 h was recorded to detect any slowly exchanging protons. The experiment was repeated by adding D_2O to the lyophilized NMR sample (molar indolicidin:DPC-d_{38} ratio of 1:200, pH* 4.6), to confirm the exchange of tryptophan indole H^N, which have a higher pH_{min} than backbone amide protons; only one-dimensional spectra were acquired.

The NMR data were processed with NMRPIPE (*20*). Resolution enhancement was achieved by apodization of the free induction decay with shifted squared sine-bell window functions. The data were zero-filled to at least twice the size prior to Fourier transformation. Spectra were baseline corrected using a fifth-order polynomial function. All chemical shifts were referenced to internal 4,4-dimethyl-4-silapentane-1-sulfonate (DSS).

NOE Data Analysis and Structure Calulation. All NMR spectra were analyzed using NMRVIEW version 4.0.5 (*21*).

[1] Abbreviations: SDS, sodium dodecyl sulfate; DPC, dodecylphosphocholine; POPC, 1-palmitoyl-2-oleoylphosphatidylcholine; POPG, 1-palmitoyl-2-oleoylphosphatidyl-DL-glycerol; headgroup-labeled tempo-PC, 1,2-dioleoyl-*sn*-glycero-3-phosphotempocholine; 5-doxyl-PC, 1-palmitoyl-2-stearoyl-5-doxyl-*sn*-glycero-3-phosphocholine; 12-doxyl-PC, 1-palmitoyl-2-stearoyl-12-doxyl-*sn*-glycero-3-phosphocholine; CMC, critical micelle concentration; CD, circular dichroism; NMR, nuclear magnetic resonance; NOESY, nuclear Overhauser effect spectroscopy; pH*, pH meter reading in D_2O; pH_{min}, pH at the minimum intrinsic exchange rate; rms, root-mean-square; TOCSY, total correlated spectroscopy; DQF-COSY, double-quantum-filtered correlated spectroscopy; NOE, nuclear Overhauser enhancement.

NOE cross-peaks were integrated in the 100 ms NOESY spectra. The NOE volumes were converted to distances, which were calibrated using the average NOE volume of all resolved geminal methylene proton cross-peaks. Each distance was converted to a distance restraint by calculating upper and lower distance bounds using the equations suggested by Hyberts et al. (*22*). Pseudoatom corrections were applied by adding 1 and 1.5 Å to the upper distance bound for unresolved methylene protons and methyl groups, respectively. No stereospecific assignments were made. Distance restraints involving resolved methylene protons were float corrected by adding 1.7 Å to the upper bound. No hydrogen bond restraints were applied. Structure calculations were performed using X-PLOR version 3.851 (*23*−*25*). Starting from a randomized template structure, 100 structures were generated using distance geometry algorithms. This was followed by 10 000 steps (0.001 ps) of simulated annealing at 1300 K and a subsequent decrease in temperature to 10 K over 10 000 steps. The refinement stage consisted of decreasing the temperature from 800 to 10 K over 50 000 steps. Of the 100 resulting structures, 16 structures converged for each micelle type with low final energies and NOE distance restraint violations of <0.4 Å. Structures were analyzed with the programs MOLMOL (*26*) and Insight II 97.0 (Molecular Simulations Inc., San Diego, CA).

Spin-Label Experiments. Three types of spin-labeled vesicles were prepared by extruding POPC, POPG, and either headgroup-labeled tempo-PC, 5-doxyl-PC, or 12-doxyl-PC at a molar ratio of 63:27:10. For fluorescence experiments, the concentrations that were used were 2 μM peptide and 0.5 mM lipid. Spin-labeled NMR samples, containing 2 mM peptide and 200 mM DPC-d_{38}, were prepared by adding small aliquots of 5-doxylstearic acid or 16-doxylstearic acid dissolved in methanol-d_4 to a concentration of 0.1−0.5 mM. The optimal spin-label concentration for large and specific effects was determined to be 0.4 mM using one-dimensional NMR spectra, which were acquired with the MLEV-17 spin-lock sequence also employed for TOCSY spectra. TOCSY spectra with a spin-lock time of 30 ms were used to compare cross-peak intensities of indolicidin before and after addition of the spin-label.

RESULTS

Interaction of Indolicidin with Detergents and Lipids. Since the conformation of indolicidin was determined using NMR in the presence of detergent, it was important to establish that the structure of this peptide formed upon binding to detergent micelles is similar to the structure when bound to phospholipid bilayers, which more closely resemble the biological membrane. Suitable methods for comparing the interaction and secondary structure of peptides in different membrane environments include fluorescence and CD spectroscopy. The fluorescence spectra of indolicidin in aqueous solution and bound to different lipid and detergent particles are shown in panels A and B of Figure 1. In the lipid-free form, indolicidin exhibited an emission maximum at 357 nm, which was equal to the tryptophan control. Binding of indolicidin to lipid vesicles (Figure 1A) effected a 10 nm blue shift of the emission maximum with a concomitant increase in intensity, indicating that the tryptophan side chains had moved into a more hydrophobic environment (*27*).

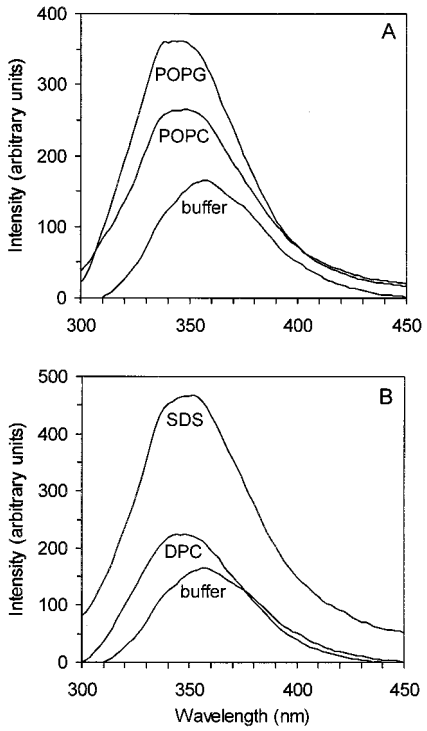

FIGURE 1: Fluorescence emission spectra of indolicidin in complexes with (A) lipid vesicles and (B) detergent micelles. The sample contained 2 μM peptide, 0.5 mM lipid or 10 mM detergent, and 10 mM HEPES buffer (pH 7.2). The emission maximum of indolicidin was 357 nm in 10 mM HEPES buffer, 347 nm for complexes with POPC and POPG, and 348 nm for complexes with DPC and SDS.

Binding of indolicidin to micelles (Figure 1B) led to similar changes in the fluorescence spectra, indicating that the environment experienced by the peptide in lipids and detergents was comparable.

The CD spectra of free and bound indolicidin are shown in panels A and B of Figure 2. In aqueous solution, the spectrum was characterized by a broad negative band at ~200 nm. This minimum is normally assigned to unordered peptides, but has also been observed for the poly-L-proline II helix (*28*) and for β-turns (*29*). No major differences were observed between the CD spectra of indolicidin bound to micelles or vesicles. When indolicidin binds to micelles (Figure 2B), the minimum at ~200 nm shifted to ~205 nm. Due to light scattering caused by large unilamellar vesicles (*30*), this effect could not be observed upon binding of indolicidin to phospholipid. In both micelles and vesicles, a second negative band appeared at ~228 nm, separated from the minimum at ~205 nm by a relative maximum at ~218 nm. The band at ~228 nm has been attributed to the tryptophan side chains of indolicidin (*9*, *12*). The rotational strength of the indole chromophore can be positive or negative depending on its orientation relative to the peptide backbone (*31*) and is thus a sensitive probe of the peptide conformation. The ellipticity of the negative band at ~228 nm for indolicidin in complexes with POPC, POPG, or DPC was identical at −8000 deg cm^2 dmol^{-1}, while it was almost twice as large (−14000 deg cm^2 dmol^{-1}) for indolicidin in complexes with SDS. These data suggest that, as compared to SDS, the conformation of indolicidin in DPC more closely resembles the conformation of the peptide bound to POPC and POPG.

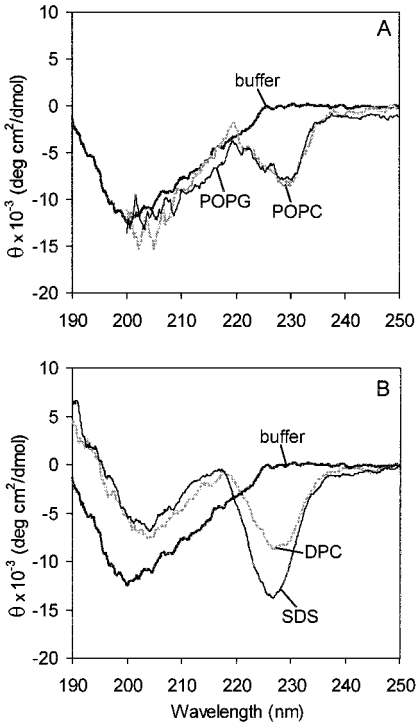

FIGURE 2: Circular dichroism spectra of indolicidin in complexes with (A) lipid vesicles and (B) detergent micelles. The sample contained 50 μM peptide, 2 mM lipid or 10 mM detergent, and 10 mM phosphate buffer (pH 7.0).

NMR Spectroscopy. To obtain optimal indolicidin−detergent complexes, free indolicidin was titrated with either DPC or SDS until no further changes in chemical shifts were observed, corresponding to a state where the peptide was maximally bound to the detergent. For indolicidin in DPC, steady state chemical shifts were reached at a molar peptide:detergent ratio of 1:100. With SDS, indolicidin formed a precipitate, which redissolved at a molar peptide:detergent ratio of 1:40; the chemical shifts remained constant upon further titration. For two-dimensional NMR studies, the indolicidin samples were prepared with an excess of detergent to minimize signal broadening due to chemical exchange. Thus, the molar peptide:detergent ratios that were employed were 1:200 for indolicidin bound to DPC and 1:120 for the peptide bound to SDS.

One-dimensional proton NMR spectra of indolicidin in aqueous solution and in complexes with DPC and SDS micelles are presented in panels A−C of Figure 3. The binding of the peptide to micelles was demonstrated by the change in proton chemical shifts compared to the aqueous phase. These chemical shift changes were seen most clearly for the indole H^N of tryptophan (residues 4, 6, 8, 9, and 11) near 10 ppm and for the backbone amide protons of residues L2, K5, W6, W8, W11, R12, and R13. In addition, the aromatic protons experienced a chemical shift dispersion upon binding of the peptide to the detergent, which was larger for indolicidin in DPC than in SDS. The H^α chemical shifts are indicators of the backbone conformation of peptides and proteins (*32*). Since the tryptophan residues in indolicidin may modify the H^α chemical shifts by ring current effects, they could not be employed for secondary structure analysis. However, the change in H^α chemical shifts between indolicidin bound to DPC or SDS was small, suggesting that the structure in these two micelle systems was similar. The

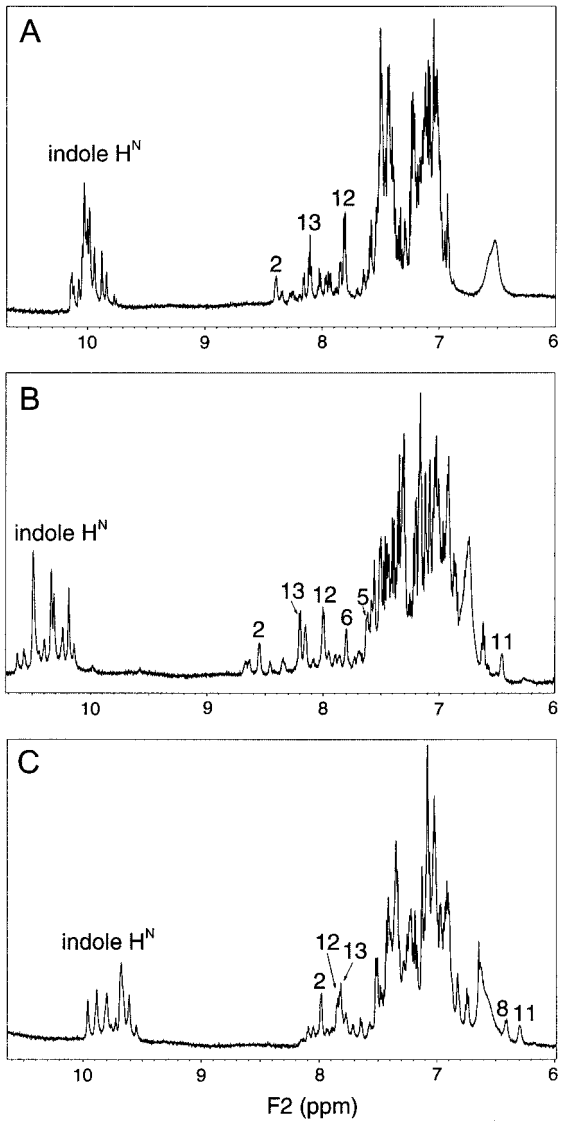

FIGURE 3: Region of one-dimensional proton NMR spectra of indolicidin (2 mM) showing the amide and aromatic resonances: (A) 10 mM phosphate buffer at pH 4.4 and 37 °C, (B) 400 mM DPC at pH 4.7 and 37 °C, and (C) 240 mM SDS at pH 4.7 and 37 °C.

largest differences were observed for residues P3 (0.15 ppm), W9 (0.10 ppm), and P10 (0.16 ppm). Due to the tryptophan contribution, these data may indicate variations in the backbone and/or side chain conformation of these or neighboring residues.

Proton Resonance Assignments. Two-dimensional NMR spectra of indolicidin were obtained at 37 °C and pH 4.7 in the presence of DPC or SDS micelles. An additional NOESY spectrum of indolicidin in DPC was obtained at 32 °C to reveal peptide resonances which were overlapped with the water resonance at 37 °C. The proton resonance assignments were made using the procedures of Wüthrich (*33*). Spin systems were identified in the TOCSY spectrum, and sequential assignments were made by $H^\alpha_i-H^N_{i+1}$ cross-peaks in the NOESY spectrum. Side chain proton assignments were confirmed with the DQF-COSY spectrum. Panels A−C of Figure 4 present portions of the TOCSY, NOESY, and DQF-COSY spectra, respectively, of indolicidin bound to DPC. Figure 4C shows the high resolution of the aromatic protons, which enabled the complete assignment of all five tryptophan

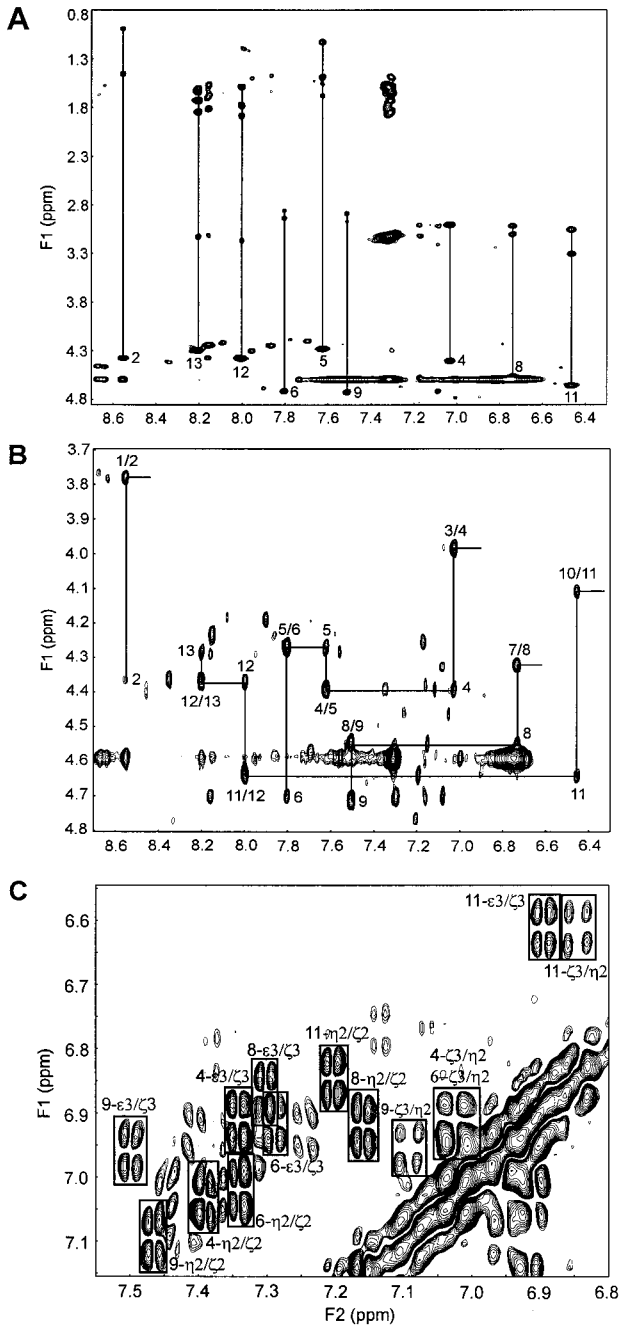

FIGURE 4: Portions of two-dimensional proton NMR spectra of indolicidin (2 mM) in DPC (400 mM) at pH 4.7 and 37 °C, illustrating resonance assignments. (A) TOCSY spectrum showing the backbone amide side chain region. Individual amino acid spin systems are indicated by vertical lines. (B) NOESY spectrum (τ_m = 100 ms) illustrating sequential amino acid residue assignments using cross-peaks between a backbone amide proton and the α-proton of the preceding residue (*υ*/*w*). Interruptions in the "sequential walk" occur at proline residues due to the absence of a backbone amide proton. (C) DQF-COSY spectrum presenting the indole ring proton assignments of tryptophan residues. Each label is composed of the residue number (*x*-) followed by the positions of the two indole ring protons (*y*/*z*) that give rise to the cross-peak.

side chains. The proton chemical shifts were deposited in the BioMagResBank (entry 4552).

It was apparent from the NMR spectra of indolicidin that, besides a major set of proton resonances, there were additional minor signals, most of which were assigned to at least the amino acid type. At the peptide termini, a doubling or tripling of the proton resonances was observed, whereas most of the central proline and tryptophan residues showed none or one additional set of signals. The chemical shifts of the additional signals could be reproduced in several sample preparations; they were present for indolicidin in aqueous solution and in the presence of detergent, and their relative intensity varied little with temperature. It has been suggested that indolicidin self-associates at >0.05 mM on the basis of the concentration-dependent intensity of the fluorescence emission (*7*). However, the one-dimensional NMR spectra of 2 and 0.04 mM indolicidin in either aqueous solution or DPC micelles were identical, suggesting that the additional signals did not arise from oligomerization. Another explanation for several sets of spin systems may be cis−trans isomerization of proline, of which indolicidin contains three. The proline residues of the major species were in the trans conformation as indicated by the presence of strong NOEs between the *δ*-protons of proline and the α-protons of the preceding residue. Cross-peaks between the α-protons of proline and the preceding residue of the minor species, indicating the *cis*-proline isomer, were not observed. Furthermore, NOE contacts between L2 and P3 for a minor species indicated the *trans*-proline isomer in both detergent systems. However, the presence of the *cis*-proline conformation in the minor species of indolicidin could not be ruled out, since NOEs may have been too weak to be observed. Evidence for the proline isomer could only be obtained for the major indolicidin species (all trans) and one minor form (*trans*-P3), whereas the proline conformations of other minor species remain unknown. Overall, the resolution of the two-dimensional NMR spectra was sufficiently high to disseminate peaks belonging to the major species from signals of the minor species (Figure 4) so that the assignment and integration of NOE cross-peaks were not affected. The structural analysis of indolicidin presented below is of the major conformation. The structure of the minor indolicidin species could not be characterized since inter-residue NOE cross-peaks were generally absent.

NOE Connectivities. The NOE cross-peak pattern between the backbone amide and α-protons for indolicidin in DPC is presented in Figure 4B. The sequential $H^{\alpha}_{i}-H^{N}_{i+1}$ cross-peaks for residues 1−6, 12, and 13 were stronger than the corresponding intraresidue $H^{\alpha}_{i}-H^{N}_{i}$ cross-peaks, approximately the same size for residues 8−11, while the sequential $H^{N}_{i}-H^{N}_{i+1}$ cross-peaks were mostly weaker. This backbone connectivity pattern is typical for an extended structure. For indolicidin in SDS, the sequential $H^{\alpha}_{i}-H^{N}_{i+1}$ cross-peaks were slightly weaker than the intraresidue $H^{\alpha}_{i}-H^{N}_{i}$ cross-peaks. In both micelle systems, the pattern of NOE connectivities for indolicidin was similar, but varied in intensity. The tryptophan side chains displayed intraresidue NOE contacts of the aromatic ring protons $H^{\delta 1}$ and $H^{\epsilon 3}$ with the α- and *β*-protons. Most inter-residue NOE connectivities were sequential. $H^{\beta}_{i}-H^{N}_{i+1}$ cross-peaks, observed throughout the sequence, were of medium and weak intensity in DPC and mostly weak in SDS. Side chain interactions between proline and the tryptophan next in sequence were manifested in both micelle systems by weak or medium $H^{\delta}_{(P)}-H^{\epsilon 3}/H^{\delta 1}_{(W)}$ contacts. The latter were especially prominent for W9 and P10. The difference in backbone orientation between indolicidin in DPC and SDS, indicated by modification of H^{α} chemical shifts of residues 9 and 10, was corroborated by the NOE connectivities in this region. The side chain contacts

Table 1: Statistics of Calculated Structures for Indolicidin in the Presence of DPC and SDS Micelles

	DPC	SDS
no. of NOE-based distance restraints	118	129
inter-residue	61	47
intraresidue	57	82
no. of NOE restraint violations >0.1 Å[a]	18 ± 1	13 ± 2
average highest NOE restraint violation (Å)	0.22 ± 0.03	0.29 ± 0.02
average total energy (kcal/mol)	56 ± 3	49 ± 4

[a] NOE restraint violations and energy values are expressed as means ± the standard deviation of 16 structures.

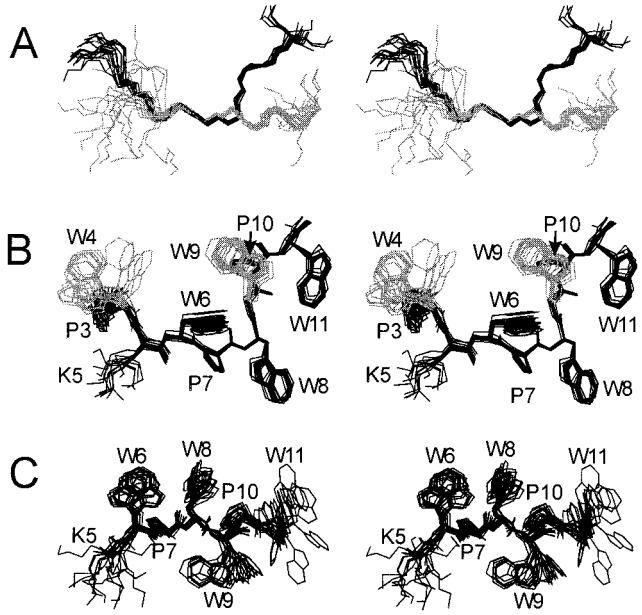

FIGURE 5: Backbone structure and side chain orientation of 16 calculated structures of indolicidin in complexes with DPC and SDS. (A) The backbone atoms (N−C^{α}−C′) of the peptide bound to DPC (black) and SDS (gray) with residues 5−7 overlaid. (B) Well-defined region of indolicidin in DPC, residues 3−11, showing all heavy atoms. The side chains of W4 and W9 are colored gray to reveal P3 and P10, respectively, behind. The aromatic rings of tryptophans 4, 8, 9, and 11 are oriented approximately parallel to the plane of the paper, while W6 extends at right angles into the back. (C) Well-defined region of indolicidin in SDS, residues 5−11, showing all heavy atoms.

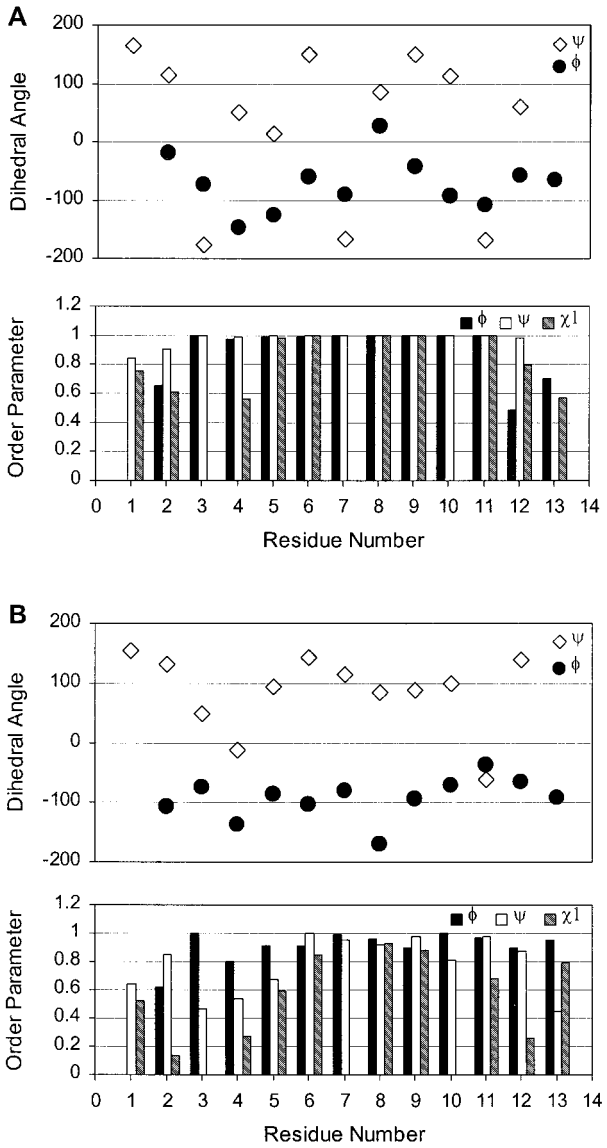

FIGURE 6: Average dihedral angles ϕ (◇) and ψ (●) as well as the respective angular order parameters (*22*) (black and white columns for ϕ and ψ, respectively, and hatched columns for χ_1) for each set of 16 structures determined for indolicidin in the presence of DPC (A) and SDS (B).

of W9 and W11 with P10, observed for indolicidin in DPC, were replaced with W8−P10 contacts in SDS.

Calculated Structure of Indolicidin. The structures of indolicidin bound to DPC or SDS micelles were calculated using 118 or 129 NOE-based distance restraints, respectively, excluding redundant restraints (Table 1). Although more distance restraints were applied to the structure of indolicidin in SDS compared to DPC, the structure in DPC was better defined than in SDS. This result is due to (i) tighter distance restraints for indolicidin in DPC than in SDS and (ii) a higher number of inter-residue restraints for the peptide in DPC than in SDS. Figure 5A shows the backbone conformation for indolicidin in DPC (black) and SDS (gray). For the peptide in DPC, the backbone was well-defined with an rms deviation to the mean coordinates of 0.31 ± 0.13 Å for residues 3−11. For indolicidin bound to SDS micelles, the backbone was ordered between residues 5 and 11 with an rms deviation of 0.49 ± 0.14 Å, whereas the four N-terminal residues were poorly defined. The side chain orientations for the well-defined regions of indolicidin bound to DPC and SDS are illustrated in panels B and C of Figure 5, respectively. For reasons similar to those noted above, the convergence of the side chains of the peptide in complexes with DPC (0.98 ± 0.49 Å) was considerably better than in complexes with SDS (1.52 ± 0.37 Å). Except for K5, the region of residues 3−11 is composed of proline and tryptophan. While the conformation of proline is covalently constrained, the conformation of tryptophan residues was defined by an average of 15 NOE-based distance restraints, thus accounting for the good precision of calculated structures.

The average dihedral angles ϕ, ψ, and χ_1 of the structures calculated for each micelle type were plotted along with the order parameters (*22*) in Figure 6. An order parameter of ~1 indicates a well-defined backbone conformation, while a small value indicates a disordered structure. The backbone dihedral angles ϕ and ψ of the well-defined regions of the peptide in both micelle systems fell within or near the

β-region of the Ramachandran plot. The structure of indolicidin bound to DPC may be described as follows. The backbone of the three N-terminal residues was extended, followed by two half-turns, consisting of residues 4−6 and 7−9, and another extended C-terminal region. The backbone atoms of residues 3−10 were approximately in one plane. The two half-turns effected a reversal in the backbone direction, orienting the N-terminus and the C-terminus toward one side of the molecule. The dihedral angles of residues W6, W9, and P10 (Figure 6) were within ±35° of an ideal type II polyproline helix ($\phi = -78°$ and $\psi = 146°$), and the side chains of residues 8−11 had a 3-fold rotational symmetry as is found in left-handed polyproline II helices (*34*). The aromatic rings of tryptophans 4, 8, 9, and 11 were roughly parallel to the backbone, while W6 extended at a right angle (Figure 5B). The structure of indolicidin bound to SDS micelles also had an extended backbone conformation (Figure 5C), but was somewhat different from the structure in DPC. The bend at residues 4−6, which was observed for indolicidin in DPC, was not well-defined in the SDS-bound peptide, since the four N-terminal residues were disordered. Furthermore, the bend at residues 7−9, observed for indolicidin in DPC, was absent in the SDS-bound molecule, which is likely due to the different NOE connectivities observed in this region. The side chain contacts of W9 and W11 with P10, observed for indolicidin in DPC, were replaced with W8−P10 contacts in SDS. Additionally, the NOE contacts between P7 and W8 were weaker for indolicidin in SDS than in DPC. Although residues W6 and P7 of indolicidin bound to SDS adopted backbone dihedral angles similar to those of a type II polyproline helix (Figure 6B), the side chains of residues 5−8 did not have 3-fold symmetry. When viewed down the backbone, the side chains of W6, W8, and P10 were overlaid on one side, occupying about one-quarter of the cross-sectional area. Similarly, the side chains of P7 and W11, and K5 and W9, were overlaid on the other side. The latter three side chains fanned out (as seen for the set of 16 structures) and constituted about three-quarters of the total cross-sectional area.

Hydrogen Bonds. The structure of peptides and proteins is frequently stabilized by hydrogen bonds formed between backbone atoms or backbone and side chain atoms (*35*). The extended conformation of indolicidin in DPC did not suggest backbone hydrogen bonds; however, the side chain indole H^N atoms were candidates for hydrogen bonds with the peptide backbone. The indole H^N atoms of W6 and W9 were within 2.5 Å of the carbonyl oxygen atoms of P7 and P10, respectively; however, the N−H−O angles were unfavorable for a strong hydrogen bond. The exchange of labile protons in indolicidin bound to DPC micelles was studied qualitatively at pH* 3.7 and 4.6, the latter pH* being closer to the pH_{min} of the tryptophan indole H^N (*36*), by adding D_2O to a lyophilized sample (*37*). Of the exchangeable protons, resolved in one-dimensional NMR spectra (Figure 3), only the amide protons of W8 and W11 were observed after 20 min at pH* 3.7. No slowly exchanging protons were detected by a TOCSY spectrum acquired 1 h after adding D_2O. At pH* 4.6, all exchangeable protons resolved in one-dimensional spectra, including the tryptophan indole H^N, exchanged within 20 min against deuterium. The absence of slowly exchanging protons suggests that the conformation of indolicidin in the presence of DPC was not stabilized by strong hydrogen bonds. The slightly retarded exchange observed for the amide protons of W8 and W11 may be due to very weak hydrogen bonding or reduction of solvent accessibility by steric hindrance (*38*). It appears that the indolicidin structure was mainly stabilized by interactions of its amino acid side chains with the micelle. In particular, tryptophan, of which indolicidin contains five, has been shown to have the highest free energy of transfer from the bilayer interface to water (1.85 kcal/mol) of all amino acid side chains (*39*). Similar conclusions have been drawn for the related peptide tritrpticin (*4*).

Charge Distribution. An electrostatic potential map of the contact surface of the calculated structure of indolicidin in DPC was computed using the MOLMOL program (*26*). Figure 7 shows the structure closest to the average of 16 calculated structures. This molecule fitted into a cell of extensions 32 Å × 25 Å × 16 Å. The charge distribution shows a hydrophobic core flanked by positively charged regions, located near both peptide termini, with three of the four charges pointed in a common direction. Four of five tryptophan indole rings packed against the peptide backbone, giving the molecule a wedge shape (Figure 7A). The surface charge composition of indolicidin in complexes with SDS was similar to that of indolicidin bound to DPC micelles. Excluding the N-terminal four residues, which were unordered, the dimensions of the molecule closest to the average structure were 25 Å × 15 Å × 15 Å. The main difference in molecular shape to the DPC-bound molecule was that the tryptophan indole rings were less ordered and extended away from the peptide backbone rather than orienting parallel to it.

Membrane Location. The wedge shape of indolicidin bound to DPC appears to be ideal for intercalation between the lipid molecules of a bilayer. When the size and charge distribution of the molecule are considered, two membrane insertions seem possible: (i) penetration into one bilayer leaflet, where the backbone (Figure 5A) is oriented like a "boat" structure with the positively charged N- and C-terminal regions directed to one side of the membrane, and (ii) a transmembrane orientation, where the two pairs of charges (Figure 7B) project onto opposite sides of the membrane. The membrane location of indolicidin was probed by NMR spectroscopy using DPC micelles containing spin-labeled fatty acids and by fluorescence spectroscopy using spin-labeled phospholipids incorporated into bilayers. Previous NMR experiments established that the nitroxide moiety of 5-doxylstearic acid was close to the surface of the DPC micelle, while the nitroxide moiety of 16-doxylstearic acid was near the micelle center (*40*). The decrease in NMR signal intensity, due to resonance line broadening, of indolicidin in DPC micelles was mostly greater for 5-doxylstearic acid than for 16-doxylstearic acid (Table 2). Furthermore, the level of quenching of the fluorescence emission of the bilayer-bound peptide was greater for spin-labels at positions 5 and 12 in the hydrocarbon chain than at the lipid headgroup (Table 2). The larger effects caused by spin-labels at positions slightly interior to the micelle or bilayer versus the effects caused by spin-labels at positions exterior or in the center of the micelle or bilayer indicate that indolicidin predominantly bound at the membrane interface, i.e., penetrating into

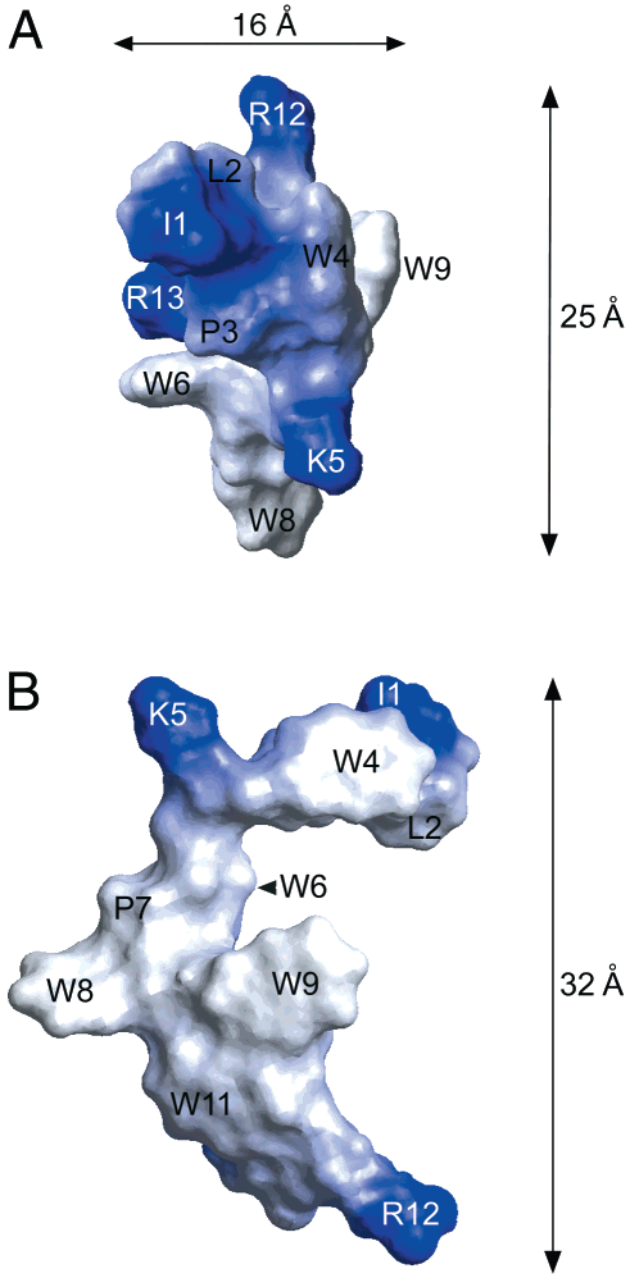

FIGURE 7: Charge distribution on the surface of indolicidin. Positive and neutral potentials are colored blue and white, respectively. Shown is the structure closest to the average of 16 structures calculated for indolicidin bound to DPC, indicating its maximal dimensions. (A) End view looking down from the N-terminus. (B) Side view with the N-terminus pointed to the top. The figure was generated using the MOLMOL program (*26*).

one bilayer leaflet. Such an orientation is likely due to the strong preference of the tryptophan indole rings for this region (*39*, *41*, *42*).

DISCUSSION

One proposed mode of antimicrobial action of indolicidin is cytoplasmic membrane perturbation by pore formation (*10*). Indolicidin induces a voltage-dependent current across planar lipid bilayers (*10*, *11*) as well as leakage of the contents of large unilamellar vesicles (*9*). However, compared to α-helical antibiotic peptides, indolicidin is less able to dissipate the bacterial inner membrane potential and forms smaller pores (*11*), yet it kills bacteria as rapidly. These

Table 2: Effects of Membrane Spin-Label Probes on ^{1}H NMR and Fluorescence Signal Intensity of Indolicidin

	% reduction in ^{1}H NMR signal intensity[a]	
residue	5-doxylstearic acid	16-doxylstearic acid
I1	–	–
L2	47	3
P3	–	–
W4	53	37
K5	39	25
W6	35	25
P7	–	–
W8	41	28
W9	35	44
P10	–	–
W11	22	0
R12	37	21
R13	20	4

	% reduction in fluorescence emission intensity[b]		
	headgroup-labeled tempo-PC	5-doxyl-PC	12-doxyl-PC
all Trp	28	51	51

[a] Reduction in TOCSY H^N-H^α cross-peak intensity using 2 mM indolicidin, 200 mM DPC-d_{38}, and 0.4 mM spin-label at pH 4.7 and 37 °C relative to the unlabeled sample. [b] Reduction in fluorescence emission intensity using 2 μM indolicidin and 0.5 mM POPC/POPG (7:3 molar ratio) large unilamellar vesicles containing 10 mol % spin-label at pH 7.2 and 22 °C relative to the unlabeled sample.

results point to a mechanism of action that is different from well-defined channel formation. Recently, indolicidin was proposed to inhibit DNA synthesis leading to filamentation in *Escherichia coli*, which would require the presence of the peptide in the cytoplasm (*43*). We have shown by spin-label experiments that an interfacial membrane location was preferred by indolicidin under our experimental conditions. However, it is intriguing that, despite only having 13 amino acids, indolicidin shares the same length with protegrin-1 (18-residue β-hairpin), alamethicin (20-residue α-helix), and magainin (23-residue α-helix), which is comparable to the thickness of a membrane. For the latter two peptides, two distinct states have been described, corresponding to orientations parallel and (at higher concentrations) perpendicular to the plane of the bilayer (*44*, *45*). We speculate that a bilayer-spanning orientation of indolicidin may be transitional and a way of redistributing the antibiotic onto the inner leaflet of the cytoplasmic membrane, from where it could diffuse to other sites in the cell. Such a traversal of the membrane would explain the bactericidal activity of indolicidin combined with a transient perturbation of planar membranes (*11*, *43*).

The determined structures of indolicidin bound to DPC and SDS micelles were somewhat different. Slight structural variations of indolicidin depending on micelle type were also suggested by the CD spectra (Figure 2B), H^α chemical shifts, and NOE connectivities. In DPC, the peptide backbone formed two half-turns, centered at residues 5 and 8, giving it a boat shape (Figure 5A,B). In the SDS-bound molecule, one of these half-turns was not well-defined, since the four N-terminal residues were disordered, while the second half-turn was absent, leading to a linearly extended backbone structure (Figure 5A,C). However, on a residue-by-residue basis, these structural differences were reduced to a ~160° backbone flip at residue 8 (Figures 5A and 6). The backbone ($N-C^\alpha-C'$) rms deviation of the average structures calcu-

lated for each micelle system was 0.32 Å for residues 5−7 and 0.50 Å for residues 9−11, but 1.36 Å for residues 5−11. The structure of indolicidin bound to SDS micelles, especially the side chains, was not as well-defined as the DPC-bound structure. While most tryptophan indole rings folded parallel to the backbone in indolicidin bound to DPC, they extended away from the backbone in the SDS-bound molecule, leaving the latter structure less compact. The CD spectrum of indolicidin in DPC most closely resembled that of the spectrum in large unilamellar vesicles of both neutral and negatively charged lipids. Due to the different headgroup charge, the zwitterionic DPC micelle [axial ratio of 1:6 (*46*)] is less spherical than the anionic SDS micelle [axial ratio of 1:2 (*47*)], and thus, its curvature would be closer to that of a liposome. The variation of the indolicidin structure with micelle type may relate to the different micelle shapes as well as to different interactions of the positively charged moieties of the peptide with the negatively charged SDS headgroup and with the zwitterionic DPC headgroup.

Recently, the structure of indolicidin in membrane environments was proposed to contain β-turns as the principal structural motifs on the basis of CD spectroscopic data (*12*). Specifically, a W6-*cis*-P7-W8 type VIa turn was modeled on the basis of two observations: (1) tryptophan exciton coupling of indolicidin bound to SDS micelles and (2) the type VI turn structure of the hexapeptide *cis*-SYPFDV in an aqueous environment, which was stabilized in part by hydrophobic stacking of aromatic and proline rings (*48*). While we could confirm β-turn structure for indolicidin in DPC, a type VI turn formed by the *cis*-proline isomer was not observed in indolicidin bound to either DPC or SDS micelles. An explanation for exciton coupling in indolicidin may still be provided by the orientation of tryptophan side chains. The theoretical maximal couplet strength has been predicted if two indole rings are in parallel planes and one ring is rotated by 45° relative to the other; Trp−Trp interactions may be significant at distances of ≤15 Å (*49*). Although the planes of W6 and W8 indole rings in indolicidin bound to SDS were nearly perpendicular, the average center−center distance was about 7 Å, possibly accounting for the observed exciton coupling.

We demonstrated here that cationic antimicrobial peptides do not need to conform to a canonical secondary structure or be amphipathic to kill bacteria. The indolicidin fold, which comprised a hydrophobic core flanked by two dispersed, positively charged regions, was qualitatively different from the recently determined structure of tritrpticin, which had a similar amino acid composition, but adopted an amphipathic structure that is more common for antimicrobial peptides (*4*). The structural differences between these two peptides, combined with the considerably higher antimicrobial activity of indolicidin (*5*) compared to tritrpticin (*50*), have significant implications for the design of novel peptide-based antibiotics. Cationic antimicrobial peptides have many highly desirable characteristics, including a broad spectrum of activity that includes most pathogenic bacteria and fungi, an ability to kill known antibiotic-resistant clinical isolates, synergy with conventional antibiotics, and an endotoxin (sepsis) neutralization activity (*2*, *51*). Our knowledge of the structure of indolicidin may provide a new lead in the design of more potent peptide antibiotics.

ACKNOWLEDGMENT

We thank Dr. Lawrence P. McIntosh (Protein Engineering Network of Centers of Excellence and Departments of Chemistry, Biochemistry, and Molecular Biology, University of British Columbia) and Dr. Robert J. Cushley (Institute of Molecular Biology and Biochemistry and Department of Chemistry, Simon Fraser University, Burnaby, BC) for assistance in the acquisition of NMR spectra.

SUPPORTING INFORMATION AVAILABLE

A portion of the NOESY spectrum of 2 mM indolicidin in 240 mM SDS at 37 °C and pH 4.7 and a region of the NOESY spectra of indolicidin in DPC and SDS micelles. This material is available free of charge via the Internet at http://pubs.acs.org.

REFERENCES

1. Boman, H. G. (1995) *Annu. Rev. Immunol. 13*, 61−92.
2. Hancock, R. E. W., and Lehrer, R. (1998) *Trends Biotechnol. 16*, 82−88.
3. Hwang, P. M., and Vogel, H. J. (1998) *Biochem. Cell. Biol. 76*, 235−246.
4. Schibli, D. J., Hwang, P. M., and Vogel, H. J. (1999) *Biochemistry 38*, 16749−16755.
5. Selsted, M. E., Novotny, M. J., Morris, W. L., Tang, Y. Q., Smith, W., and Cullor, J. S. (1992) *J. Biol. Chem. 267*, 4292−4295.
6. Aley, S. B., Zimmerman, M., Hetsko, M., Selsted, M. E., and Gillin, F. D. (1994) *Infect. Immun. 62*, 5397−5403.
7. Ahmad, I., Perkins, W. R., Lupan, D. M., Selsted, M. E., and Janoff, A. S. (1995) *Biochim. Biophys. Acta 1237*, 109−114.
8. Robinson, W. E., Jr., McDougall, B., Tran, D., and Selsted, M. E. (1998) *J. Leukocyte Biol. 63*, 94−100.
9. Ladokhin, A. S., Selsted, M. E., and White, S. H. (1997) *Biophys. J. 72*, 794−805.
10. Falla, T. J., Karunaratne, D. N., and Hancock, R. E. W. (1996) *J. Biol. Chem. 271*, 19298−19303.
11. Wu, M., Maier, E., Benz, R., and Hancock, R. E. (1999) *Biochemistry 38*, 7235−7242.
12. Ladokhin, A. S., Selsted, M. E., and White, S. H. (1999) *Biochemistry 38*, 12313−12319.
13. Henry, G. D., and Sykes, B. D. (1994) *Methods Enzymol. 239*, 515−535.
14. Braunschweiler, L., and Ernst, R. R. (1983) *J. Magn. Reson. 53*, 521−528.
15. Jeener, J., Meier, B. H., Bachmann, P., and Ernst, R. R. (1979) *J. Chem. Phys. 71*, 4546−4553.
16. Rance, M., Sorensen, O. W., Bodenhausen, G., Wagner, G., Ernst, R. R., and Wüthrich, K. (1983) *Biochem. Biophys. Res. Commun. 117*, 479−485.
17. Piotto, M., Saudek, V., and Sklenar, V. (1992) *J. Biomol. NMR 2*, 661−665.
18. Sklenar, V., Piotto, M., Leppik, R., and Saudek, V. (1993) *J. Magn. Reson. A102*, 241−245.
19. Bax, A., and Davis, D. G. (1985) *J. Magn. Reson. 65*, 355−360.
20. Delaglio, F., Grzesiek, S., Vuister, G. W., Zhu, G., Pfeifer, J., and Bax, A. (1995) *J. Biomol. NMR 6*, 277−293.
21. Johnson, B. A., and Blevins, R. A. (1994) *J. Biomol. NMR 4*, 603−614.
22. Hyberts, S. G., Goldberg, M. S., Havel, T. F., and Wagner, G. (1992) *Protein Sci. 1*, 736−751.
23. Kuszewski, J., Nilges, M., and Brunger, A. T. (1992) *J. Biomol. NMR 2*, 33−56.
24. Nilges, M., Clore, G. M., and Gronenborn, A. M. (1988) *FEBS Lett. 229*, 317−324.
25. Nilges, M., Kuszewski, J., and Brunger, A. T. (1991) in *Computational Aspects of the Study of Biological Macromolecules by NMR*, Plenum Press, New York.

26. Koradi, R., Billeter, M., and Wüthrich, K. (1996) *J. Mol. Graphics 14*, 51−55.
27. Lakowicz, J. R. (1983) *Principles of fluorescence spectroscopy*, Plenum Press, New York.
28. Bovey, F. A., and Hood, F. P. (1967) *Biopolymers 5*, 915−919.
29. Perczel, A. (1991) *J. Am. Chem. Soc. 113*, 9772−9784.
30. Wallace, B. A., and Mao, D. (1984) *Anal. Biochem. 142*, 317−328.
31. Woody, R. W. (1994) *Eur. Biophys. J. 23*, 253−262.
32. Wishart, D. S., Sykes, B. D., and Richards, F. M. (1991) *J. Mol. Biol. 222*, 311−333.
33. Wuthrich, K. (1986) *NMR of Proteins and Nucleic Acids*, Wiley, New York.
34. Cowan, P. M., and McGawin, S. (1955) *Nature 176*, 501−503.
35. Baker, E. N., and Hubbard, R. E. (1984) *Prog. Biophys. Mol. Biol. 44*, 97−179.
36. O'Neil, J. D., and Sykes, B. D. (1989) *Biochemistry 28*, 6736−6745.
37. Wuthrich, K., and Wagner, G. (1979) *J. Mol. Biol. 130*, 1−18.
38. Bai, Y., Milne, J. S., Mayne, L., and Englander, S. W. (1993) *Proteins 17*, 75−86.
39. Wimley, W. C., and White, S. H. (1996) *Nat. Struct. Biol. 3*, 842−848.
40. Brown, L. R., Bosch, C., and Wuthrich, K. (1981) *Biochim. Biophys. Acta 642*, 296−312.
41. Yau, W. M., Wimley, W. C., Gawrisch, K., and White, S. H. (1998) *Biochemistry 37*, 14713−14718.
42. Braun, P., and von Heijne, G. (1999) *Biochemistry 38*, 9778−9782.
43. Subbalakshmi, C., and Sitaram, N. (1998) *FEMS Microbiol. Lett. 160*, 91−96.
44. Huang, H. W., and Wu, Y. (1991) *Biophys. J. 60*, 1079−1087.
45. Ludtke, S. J., He, K., Wu, Y., and Huang, H. W. (1994) *Biochim. Biophys. Acta 1190*, 181−184.
46. Lauterwein, J., Bosch, C., Brown, L. R., and Wuthrich, K. (1979) *Biochim. Biophys. Acta 556*, 244−264.
47. Tanford, C., and Reynolds, J. A. (1976) *Biochim. Biophys. Acta 457*, 133−170.
48. Yao, J., Dyson, H. J., and Wright, P. E. (1994) *J. Mol. Biol. 243*, 754−766.
49. Grishina, I. B., and Woody, R. W. (1994) *Faraday Discuss. 99*, 245−262.
50. Lawyer, C., Pai, S., Watabe, M., Borgia, P., Mashimo, T., Eagleton, L., and Watabe, K. (1996) *FEBS Lett. 390*, 95−98.
51. Hancock, R. E. (1997) *Lancet 349*, 418−422.

BI000714M